Percolation analysis for estimating the maximum size of particles passing through nanosphere membranes

Emily V. White,[1] David Fullwood,[2] Kenneth M. Golden,[3] and Ilya Zharov[1]
[1]*Department of Chemistry, University of Utah, Salt Lake City, Utah 84112, USA*
[2]*Department of Mechanical Engineering, Brigham Young University, Provo, Utah 84602, USA*
[3]*Department of Mathematics, University of Utah, Salt Lake City, Utah 84112-0090, USA*

(Received 31 October 2018; published 28 February 2019)

Percolation theory can be used to study the flow-related properties of various porous systems. In particular, recently developed membranes from silica nanoparticles with surface grafted polymer brushes represent a quintessential hard-sphere soft-shell system for which fluid-flow behavior can be illuminated via a percolation framework. However, a critical parameter in membrane design involves the maximum pass-through size of particles. While percolation theory considers path connectedness of a system, little explicit consideration is given to the size of the paths that traverse the space. This paper employs a hard-sphere soft-shell percolation model to investigate maximum particle pass-through size of membranes. A pixelated (as opposed to continuous) representation of the geometry is created, and combined with readily available homology software to analyze percolation behavior. The model is validated against previously published results. For a given sphere volume fraction, the maximum diameter of a percolating path is determined by applying iterative dilations to the spheres until the percolation threshold is reached. A simple approximate relationship between maximum particle size and sphere volume fraction is derived for application to membrane design. Experimental particle cutoff size results for the polymer modified silica nanoparticle membranes were used as a partial verification of the model created in this paper. The presence of a distribution of sphere sizes (naturally created by the manufacturing process) is found to have negligible effect, compared to results for a single sphere size.

DOI: 10.1103/PhysRevE.99.022904

I. INTRODUCTION

Hairy nanoparticle (HNP) membranes, composed of a hard-sphere silica core with polymeric brushes stretching from the surface, represent a new class of low-cost, self-assembled nanoporous membranes that can be used to separate nanoscale moieties, such as viruses, nanoparticles, and biomacromolecules [1]. An scanning electron microscopy (SEM) image of a dry HNP membrane is shown in Fig. 1(a), and a figurative illustration of the structure of the particles is shown in Fig. 1(b). The size of the pores in the membrane can be altered by changing the diameter of the silica spheres and the length of the polymer brushes. Predicting the size of particulates that can pass between the HNPs that comprise the membrane is difficult; the membranes are not ordered and the silica sphere sizes and polymer brush lengths can vary greatly. Having the ability to estimate this maximum particle size (also known as the pore size cutoff) is a vital capability for assessing various membrane separation processes.

Many studies have investigated path connectedness across the solid phase of a system of spheres. The case of randomly placed spheres that are allowed to fully overlap represents a particularly common, and related, example [2–4]. The HNP membranes present a hard-sphere (the silica core) soft-shell (the polymer brush) system, where only partial "overlap" of neighboring spheres occurs via interdigitation or deformation of the polymer brushes. Percolation across the solid phases of such hard-sphere soft-shell systems has also been assessed in several studies (e.g., [5]). However, for the study of membrane filtration properties, the pathwise connectedness of the fluid phase is of more interest; a smaller number of studies have analyzed percolation of the fluid in spherical particle networks [6,7]. But little analysis has been undertaken to determine the maximum radius of a particle that can pass through the sphere network. Saxton [8] has investigated this very topic for two-dimensional systems of spheres with varying degrees of overlap, and there have been a few other forays into "critical path analysis" and pore size parameters, which are briefly reviewed below. In this paper, we extend previous continuum percolation studies in order to determine the maximum particle radius that can pass through three-dimensional (3D) membranes composed of hard silica spheres with soft polymer coatings. A range of ratios of hard-sphere radii to soft-shell thicknesses is considered, along with different distributions of sphere radii.

While the results apply to numerous situations involving fluid flow between particles, the specific application of interest involves ultrafiltration HNP membranes. The hairy nanoparticles are formed by growing polymer "hairs" on the surface of silica spheres. The details of membrane formation and cutoff size analysis are given in the method section below. The results from the cutoff experiments are compared with the model created in this paper to determine whether the mathematical representation of membrane cutoff size is accurate for this system of randomly packed hairy nanoparticles.

Geometrical approximations are often used to estimate the pore sizes between the spheres in membranes. In the subsequent section, we briefly review these methods, and

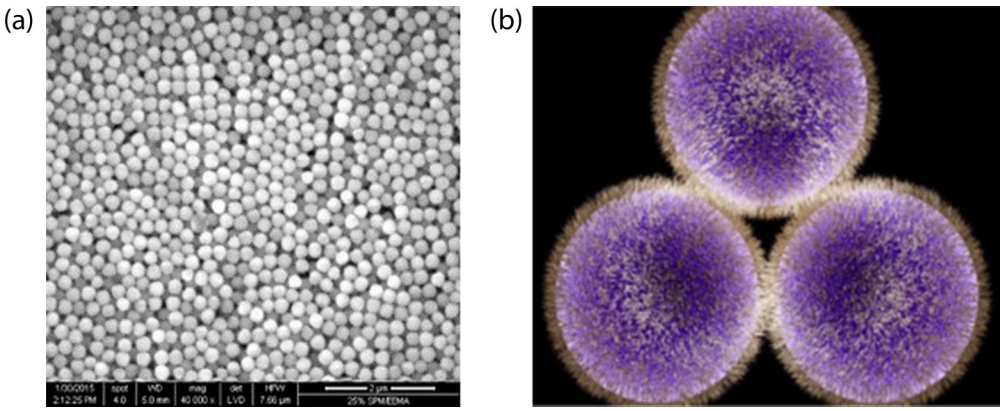

FIG. 1. (a) SEM image of the hairy nanoparticle membrane created via deposition method. (b) Representation of the hypothesized pore structure within the hairy nanoparticle membrane. Reprinted with permission from Ref. [1].

then summarize prior work in the field of percolation that lays the foundation for the current paper. This paper then develops a percolation framework to determine the maximum sized particle that could pass through a randomly packed hard-core soft-shell particle system. A 3D lattice structure approximates the actual physical membrane, with adequacy of resolution being verified against published results of percolation thresholds for overlapping spheres. The results and underlying numerical framework can be applied to a range of physical systems involving fluid flow between hard-sphere soft-shell distributions with a wide range of characteristics.

A. Analytical bounds and estimates

Crude estimates of the maximum particle size that can pass through a membrane of spheres can be determined by assuming a face-centered cubic arrangement of spheres (i.e., close packed). This configuration yields the size of the largest spherical particle that could pass through a system of hard spheres, of a given constant radius, at their maximum volume fraction [Fig. 2(a)]. For situations where the volume fraction is lower, the distance between the spheres can be scaled to achieve the correct volume fraction, leading to an estimate of particle size that scales with volume fraction [Fig. 2(b)]. A soft shell can also be included in these simple geometrical approximations [Fig. 2(c)].

Hence, for close-packed equally sized spheres of radius r_h, any particle smaller than r_p, derived in Eq. (1), can pass between the spheres:

$$r_p = \frac{r_h}{\cos(30)} - r_h = 0.1547 r_h. \tag{1}$$

Similarly, for spheres of radius r_h that are equally spaced in a membrane with volume fraction $v < 0.7405$, any particle of size less than r_p can pass between the spheres, as depicted in Eq. (2):

$$r_p = \left(\frac{0.7405}{v}\right)^{1/3} 0.1547 r_h. \tag{2}$$

Similarly, if the hard spheres of radius r_h have a soft shell of thickness d, and the soft shells overlap by a total distance of $2(d - d_i)$ [see Fig. 2(c); there is no assumed attraction between the spheres, so the soft shells can partially or fully overlap], then a particle with radius smaller than r_p, calculated in Eq. (3), can pass between the spheres:

$$r_p = \frac{r_h + d_i}{\cos(30)} - r_h - d = 0.1547 r_h + 1.1547 d_i - d \tag{3}$$

Note that all three derived estimates will clearly be lower than the real maximum particle size that can pass through random systems, since any deviation from equal spacing between the spheres will open up a wider passage for particles to be transported through. As will be shown below, such analytical estimates, based upon simple geometries, provide reasonable assessments of pore size when the volume fraction of spheres is close to the close-packed volume fraction of 0.7405. For lower volume fractions, the estimates deteriorate considerably.

B. Percolation theory

The basic problem of determining an accurate size of particles that can pass through a membrane is equivalent to determining the maximum radius of a cylindrical cross section of a snaking pipe or pathway through the network that connects one side to the other. In percolation theory, the underlying problem more typically involves determining whether there is a connected path from one side of a structure to the other, without necessarily considering the dimension (such as the radius) of such a path. The volume fraction at which an infinite connected path appears in the system is termed the percolation threshold.

The percolation threshold of overlapping spheres has been studied by many authors. Most studies have focused on percolating paths that traverse the spheres, rather than the voids between the spheres [4]. However, a small number of papers have analyzed pathways through the interstitial fluid, which is more appropriate for our membrane system. Priour [6] utilized virtual tracer particles to determine pathways through voids within the sphere system, along with a Monte Carlo calculation to determine the percolation threshold of randomly placed overlapping spheres. He reports that for various system sizes the critical volume fraction of voids is 0.0317 ± 0.0004. Rintoul [7] also studied percolation through a system of overlapping spheres using an approach based on Voronoi diagrams

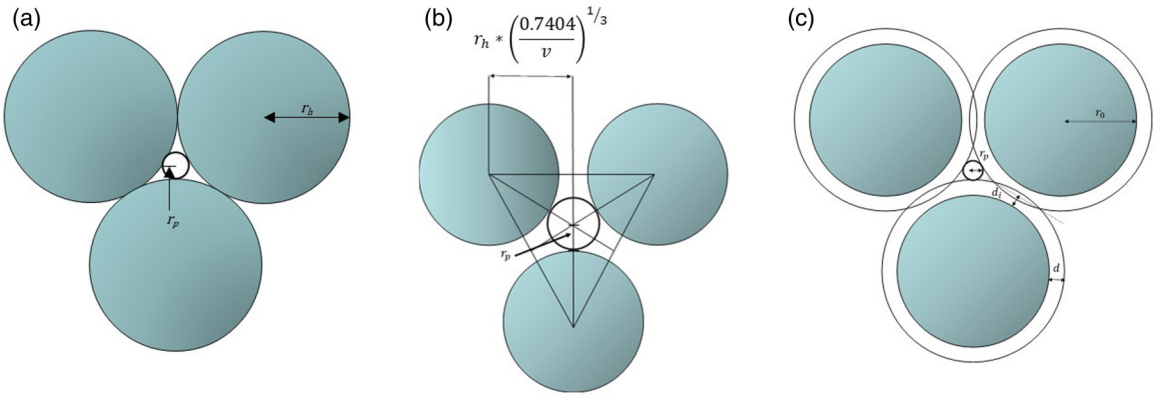

FIG. 2. Geometric models for predicting the pore size between spheres in a (a) close-packed hard-sphere system, (b) hard-sphere system with the desired volume fraction, and (c) hard-core soft-shell system.

and binary search. This work also demonstrated that the percolation threshold in a bidisperse system (i.e., composed of two different sizes of spheres) is slightly different from that of a monodisperse system. The percolation threshold found for the monodisperse model was 0.0301 ± 0.0003 (similar to that found by Priour [6]), and the threshold for a distribution of two-sized spheres had a value of 0.0287 ± 0.0005.

Martys *et al.* reported on overlapping and nonoverlapping random sphere models using a universal scaling ansatz to calculate critical porosity [9]. The porosity in these models was controlled by changing the sphere radius; increasing the radius effectively decreases the porosity. The percolation threshold was found to be ∼0.03 for all random overlapping sphere simulations, consistent with the work of Priour [6] and Rintoul [7].

Hard-core soft-shell models and their percolation properties have also been researched by several groups. Oladewa studied hard-core soft-shell spheres using Monte Carlo simulations for both uniform and random size distributions [10]. For a monodisperse system, the difference between the soft-core and hard-core soft-shell models decreases as the sphere radius increases, and eventually becomes negligible. For smaller sphere radii, a larger number of spheres is required for the hard-core soft-shell model to span the model cell. Calculations with random size distributions within the hard-core soft-shell model displayed a linear decrease in the percolation thresholds as the maximum allowed sphere size increased 10–30% from the original 264-nm diameter.

While the "diameter" of percolating paths is not typically considered in these papers, several studies have used critical path analysis to assess material properties such as electrical conductivity and fluid permeability in media with a wide range of local conductance. For example, Ambegaokar *et al.* [11] hypothesized that transport through such a medium is dominated by the presence of a certain minimal critical conductance—or *bottleneck*—that controls flow through key percolating pathways. This was proven to be correct by Golden and Kozlov [12]. Such studies complement the aim of our paper, which is to determine critical volume fractions when paths of certain minimal diameter percolate any given medium. Once these critical volume fractions have been determined, the scaling laws presented in the critical path analysis studies might be used to determine fluid permeability (for example) in the region of the percolation threshold.

Others have built upon the Ambegaokar *et al.* [11] conjecture for the hard-sphere model, to demonstrate a relationship between a pore size characteristic length (that corresponds to the largest sphere that can pass through the pore space) and sample permeability plus electrical conductivity of the sample saturated with a conductive fluid [13,14]. Finally, a model by Johnson, Koplik, and Schwartz [15] developed a relationship between a characteristic pore size parameter, Λ, and the volume-to-surface-area ratio of pore space in the sample, $\frac{V_p}{S_p}$:

$$\Lambda = \frac{2}{m(\phi)} \frac{V_p}{S_p}, \tag{4}$$

where m is a function of sample porosity, ϕ, which has been shown to take an approximately constant value of 1.5 for porosity values of $0.2 \leqslant \phi \leqslant 1$ [16,17]. We will refer to this model as the JKS model, and will compare the results of this simple relationship with detailed numerical calculations.

II. METHOD

A. Membrane formation

Silica nanoparticles of a consistent size were created using the Stöber and Fink method [18]. These were then modified to create hairy nanoparticles by growing polymer hairs on the surface of silica spheres [19,20]. Various polymers can be grown using atom transfer radical polymerization to achieve different membrane selectivity mechanisms, but for the purpose of this paper a neutral polymer, poly(2-ehydroxyethyl methacrylate), was used. The polymer length can be estimated by calculating the degree of polymerization (DP) or number of monomers per unit surface area at a certain grafting density (in this case $0.2\,\mathrm{nm}^{-2}$). This value is then taken to the power of 0.5 to arrive at an estimate of the polymer brush lengths at low grafting density [21]. In this paper, two brush lengths were produced and analyzed; the longer brushes are estimated to be 22 ± 5 nm in length (DP498 ± 53) and the shorter brushes are estimated at 10 ± 2 nm (DP106 ± 11). Membranes were created by suspending the polymer-modified particles in an ethanol or water solution and depositing them onto nylon

supports using a dead-end filtration cell at a pressure of 1 atm [see Fig. 1(a) for an SEM image of the final membrane]. The membranes remain in the ethanol or water solution for actual application.

Filtration size cutoff values for membranes were determined using dendrimer molecules of 6-nm diameter and gold nanoparticles of 20- and 40-nm diameter; particles of known size were suspended in water and pushed through the membrane to determine the maximum size of particulates able to pass between the spheres. The presence or absence of particles of a specific size in the filtrate was confirmed by dynamic light scattering and UV-Vis spectroscopy. The results from this cutoff experiment are compared with the model created in this paper.

B. Percolation model

Due to the nature of the geometry of the fluid cavity between spheres, with extremely constricted and narrow channels near points of contact, previous studies have generally relied upon continuum rather than pixelated or lattice-based representations of the sphere and fluid complex. However, the ease of handling lattice or array type structures, and the related available tools to check percolation behavior, make such a model extremely attractive if the desired resolution can be achieved. Furthermore, the rapid increase in computer power has made the scale of such a model, with the combined requirements of large size and high resolution, tractable. Hence, a discrete type of model will be assumed for the membrane geometry in this paper, resulting in a highly accessible percolation model that might be applied to many other situations.

The nanosphere membrane is assumed to be composed of a hard-sphere or soft-shell type structure. Conceptually, the radius of the "hard sphere" may be assumed to be the radius of the silica spheres, or it may include part of the polymer brush if it is determined that deformation or interdigitization of the brush only allows a certain amount of overlap for the brush shell. The soft-shell thickness is then given by the overlap allowed for polymer brushes on neighboring spheres.

An array of such spheres was set up by evenly spacing the spheres in a cubic, close-packed array, and then expanding the cube dimensions evenly while leaving the sphere diameters constant, to achieve the target volume fraction. Periodic boundary conditions were applied on each face of the cube. The number of spheres in each dimension was selected to approximate an infinite membrane; in practice this was achieved by increasing the number of spheres until the percolation threshold for a system of overlapping spheres matched published values of $\sim$0.97. Once the grid of spheres was in place, spheres were selected randomly, and then shifted randomly within their local neighborhood, while maintaining the constraint that nearby spheres could not overlap by more than the soft-shell thickness. This was repeated until every sphere had shifted approximately 500 times to ensure a random placement, as shown in Fig. 3. The random nature of the resultant positioning was checked by comparing the sphere percolation threshold with published values. The overall approach to defining the geometry was later found to be very close to method "G" described by Martys *et al.* [9].

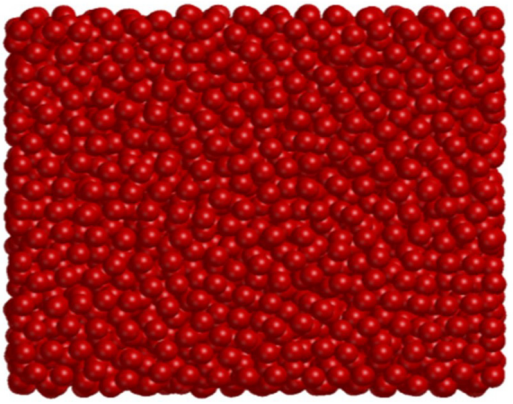

FIG. 3. Random placement of homogenously sized hard spheres.

The presence of a percolating path was checked using homology software, CHOMP [22], based on a previously hypothesized relationship between the system's homology and percolative characteristics [23]. CHOMP considers two pixels to be connected if a face or a corner is shared, which is equivalent to next-nearest-neighbor percolation. For example, if only shared faces were considered (as is the case in many models), there are six connected neighbors per pixel, whereas if both faces and corners are considered to constitute a connection 14 connected neighbors are present per pixel. In homology notation, the first two Betti numbers, β_0 and β_1, represent the number of connected components and the number of loops within a structure, respectively. For example, a donut placed in a box, X, is made of a single connected component $[\beta_0(X) = 1]$ and a single loop $[\beta_1(X) = 1]$; a "figure 8" is also made of a single connected component but has two loops $[\beta_1(X) = 2]$. The relative homology captures the homology characteristics of a space X relative to a subspace, A; for example, $\beta_1(X, A)$ is the number of linearly independent loops or independent paths that begin and end in A (see [23] for a more detailed description).

Imagine a pixelated image, X, of two phases (one that conducts, and the other that does not); define a connected top border, A, and a connected bottom border, B. The number of independent closed loops in this space is given by $\beta_1(X + A + B)$. Now add a (percolating) path that connects the top and bottom borders; this will not increase the number of closed loops. However, if A and B are now connected (e.g., by bending X until A and B sit on top of each other), and shrunk to a point, the top and bottom of the percolating path are now connected, thus increasing the number of closed loops. The number of independent closed loops in this new space is given by the relative homology $\beta_1(X + A + B,\ A + B)$. Hence, one may determine whether percolation has occurred between the top and bottom borders by considering

$$\beta_1(X + A + B,\ A + B) - \beta_1(X + A + B) \times \begin{cases} >0 & \text{if percolation has occured} \\ =0 & \text{if percolation has not occcured} \end{cases}. \tag{5}$$

In practice, for typical systems, there is only one percolating path, so the left-hand side of Eq. (5) takes the value 1 when percolation has occurred or zero when it has not.

For the given system of spheres, the radius of the largest percolating particle is then calculated by dilating each sphere (allowing the dilated sphere to overlap with nearby spheres) until a percolating path through the structure no longer exists. At this point the radius of dilation is equal to the largest particle that could pass through the original structure. If the dilation thickness at the point of final blockage is d, then the nearest that any point on the path can be to an original undilated sphere is d (if this was not the case, and a point on the path were closer than d to a particular sphere, then the dilation process would have engulfed the point at some earlier dilation time). Therefore, a spherical particle of radius d is the largest particle that could pass through the undilated sphere structure. A summary of the numerical process for determining the dilation required to reach the percolation threshold (and, hence, the maximum particle size) can be found in Fig. 4.

If the fluid and void percolation threshold of all hard-sphere or softshell models is known (i.e., for all ratios of hard-sphere radii and soft-shell thicknesses, etc.), then the dilation process need only continue until the resultant hard-sphere or soft-shell model (incorporating the dilation thickness into the softshell total thickness) reaches the relevant percolation threshold; i.e., the percolative state of the system does not need to be checked, speeding up the calculations tremendously. However, while previous work indicates a percolation threshold in the region of 0.97 sphere volume fraction, this needed to be checked for a wider set of cases than previously reported. Hence, the percolation threshold was calculated across the range of volume fractions, sphere sizes, and soft-shell thicknesses, and for a distribution of sphere sizes in a single structure. Based upon previous literature, it was hypothesized that the percolation threshold would be fairly insensitive to the sphere radius or soft-shell thickness and to the sphere size distribution, which should result in a void percolation threshold close to 3% (i.e., 97% volume fraction of spheres).

As discussed above, the formation of silica spheres via the Stöber and Fink method [18] results in a distribution of sphere sizes (e.g., one batch was characterized with a sphere size of 330 ± 30 nm); i.e., percolation results for a constant sphere size might not be valid for different batches. In order to obtain a more accurate representation of the real membrane, a range of sphere sizes must be used within the model. A model with a distribution of sphere sizes has not been well explored in the literature; Rintoul [7] created a system of spheres with two different sizes that led to an increase in the percolation threshold, but as far as we are aware a normal (or Gaussian) distribution of spheres has not been studied. For this paper, this was done by assuming a normal distribution of sphere sizes of mean diameter 30 and a standard deviation of 4 pixels; these values are analogous to silica particles of 300 nm with a standard deviation of 40 nm (fairly close to the actual standard deviation determined for the formed spheres). The standard deviation was chosen to be larger than the actual measured values from several batches, to evaluate how large of an effect the sphere size distribution has on the percolation threshold and related maximum particle size. An example of randomly placed spheres for the normal size distribution system is shown in Fig. 5, along with a representation of the same system with soft shells added to the hard spheres.

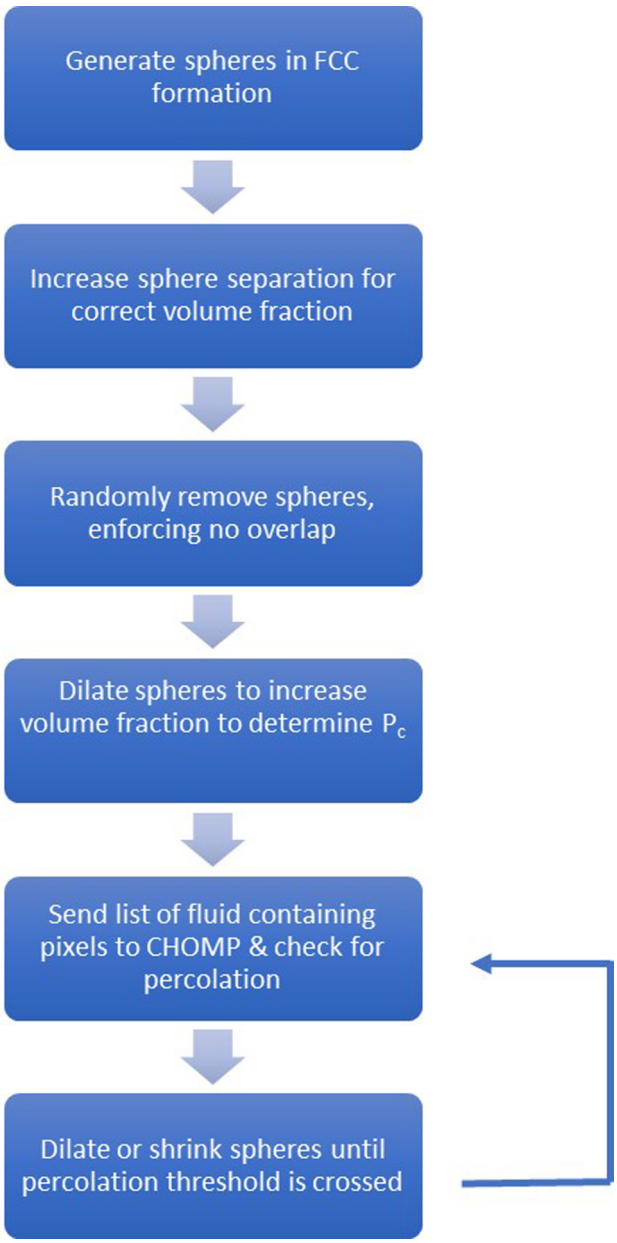

FIG. 4. Flow chart of the method of modeling percolation through a system of random spheres. P_c is the percolation threshold.

III. RESULTS AND DISCUSSION

As described above, the initial datum required to determine maximum particle radius that could pass through a membrane the soft-shell thickness required to block fluid flow in arrays of hard spheres across a range of volume fractions. Various sphere sizes, r_h, and array sizes were modeled in order to determine the required system dimensions to achieve reasonable resolution when using a model with such a discrete (lattice type) geometry. The final results are based upon spheres with a 30-pixel diameter and an initial periodic array of 24 spheres in each direction, i.e., ~14 000 spheres. The total size of the box

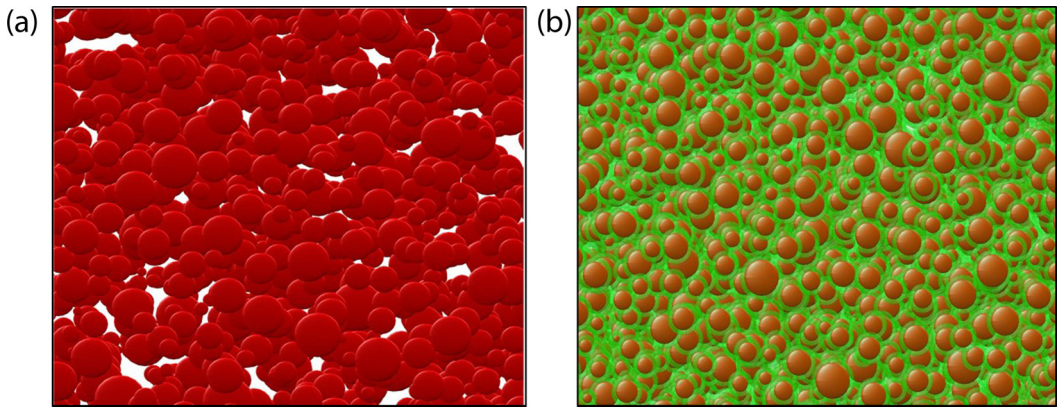

FIG. 5. Image of the normal distribution of sizes in (a) the hard-sphere system and (b) the soft-shell hard-core system; the soft shell is shown in green.

containing the spheres is dependent upon the volume fraction of spheres; for a close-packed arrangement (volume fraction of 0.7405) the box has a side length of around 360 pixels, for a total number of $\sim 47 \times 10^6$ pixels; for a volume fraction of hard spheres of 0.1, the box has a side length of approximately 700 pixels, for a total of around 340×10^6 pixels.

The selection of 30 pixels for the sphere diameters was based upon a sensitivity study. Diameter sizes of 30, 20, and 10 pixels were chosen to assess the change in the apparent critical volume fraction as a result of sphere size. As depicted in Fig. 6, the critical volume fraction decreases with decreasing sphere diameter. This is expected; as the resolution worsens it is harder for the pixelated geometry to represent the narrow regions of free space between spheres. Above the diameter of 20 pixels, the percolation threshold results were within 0.5% of the expected value of 0.97; hence, the diameter of 30 pixels was deemed acceptable.

Based upon these model parameters, the volume fraction of hard spheres plus soft shell that occurred at the percolation threshold for fluid flow between the spheres was calculated to be 0.9662 with a standard deviation of 0.0035. This is within 0.4% of published results, that lie between 0.97 and 0.9699 as discussed above, leading us to conclude that the pixelated geometry gives accurate results at the selected resolution.

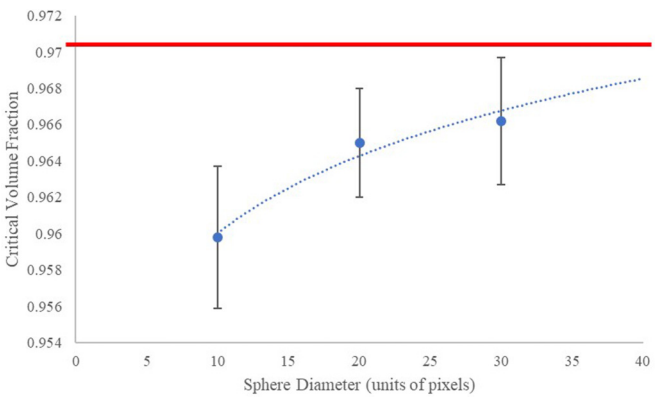

FIG. 6. Graph displaying the change in calculated critical volume fraction as a function of the sphere diameter; the target value is shown as the bold red line.

For a given hard-sphere volume fraction the soft-shell thickness required to block fluid flow (or, equivalently, the maximum particle size that can pass through the sphere array) can be directly calculated by increasing the shell thickness until percolation stops or until the known percolation threshold is reached. Tests across a wide range of volume fractions and (constant) sphere sizes confirmed that the critical sphere volume fraction is approximately 0.97 and is constant. This is consistent with published results. However, as discussed, it was not known how a distribution of sphere sizes might affect these results.

A system with a normal distribution of sphere sizes (mean diameter of 30 ± 4 pixels) was studied to better represent the real sphere distribution within membranes. Tests across this set of spheres yielded a critical volume fraction of 0.9663 ± 0.0027. This is also consistent with a previous study of a binary sized sphere system, which also yielded a slight (0.002) increase in critical volume fraction from the monodisperse calculations [7]. However, since the slight increase is within one standard deviation, it should be kept in mind that this increase is statistically insignificant. The principal result is that the distribution of sphere sizes may increase the percolation threshold, but only very slightly; assuming a threshold of 0.97 would be a reasonable estimate for both the single sized spheres and the normal distribution of spheres.

Figure 7 presents the relationship between hard-sphere volume fraction and total volume fraction from the numerical model, for a range of soft-shell thicknesses. Based upon a constant percolation threshold, this graph can be used to determine the required dimensions of percolating paths. The maximum percolating particle radius (or, equivalently, the maximum percolating path radius) can be determined from the data in Fig. 7 by extracting the soft-shell thickness required to block percolation at 0.97 total volume fraction. The results are shown in Fig. 8; the curve fit to the data points takes the form of Eq. (6). In this equation, t_s is the soft-shell thickness required to achieve the percolation threshold for a hard-sphere radius of r_h at a volume fraction of V_h.:

$$\frac{t_s}{r_h} = 1.1579 V_h^{-0.440} - 1.1678. \tag{6}$$

At the close-packed volume fraction of 0.7405, the soft-shell thickness to block percolation is $0.1547 r_h$, as was also

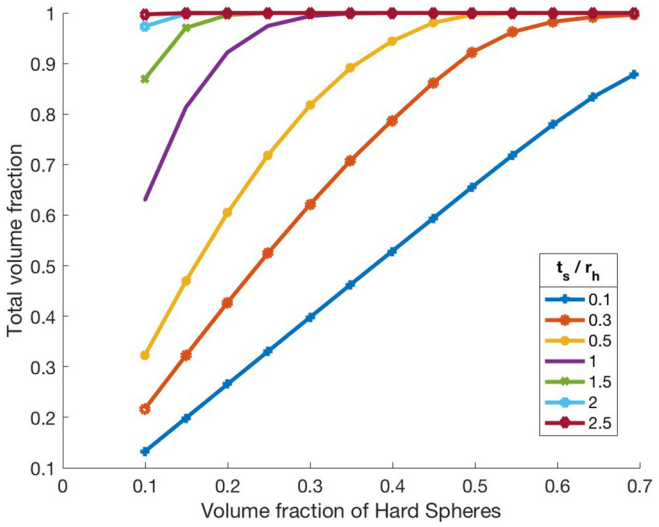

FIG. 7. Graph of the volume fraction of hard spheres vs the total volume fraction of the hard-core soft-shell system for a range of soft-shell thicknesses.

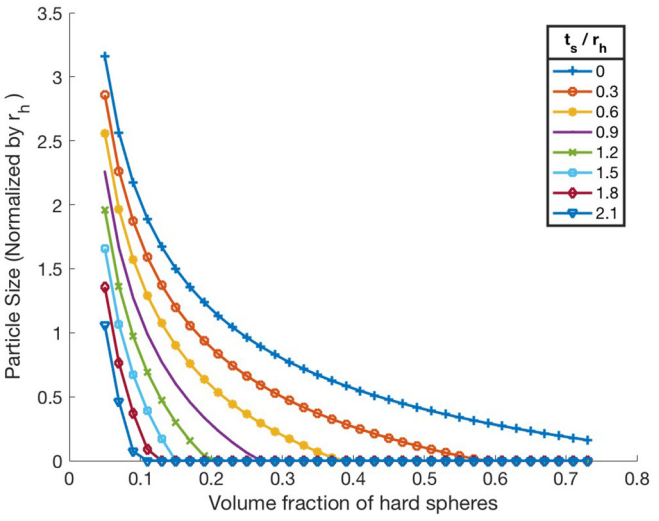

FIG. 9. Maximum particle size that can percolate through the system as a function of the volume fraction of hard spheres for a range of soft-shell thicknesses.

illustrated in Fig. 2. At the other extreme, when the hard-sphere volume fraction drops to 0.1, a soft-shell radius of $2r_h$ would be required to block percolation (from Fig. 8), and hence a particle of that size could pass along a percolating path.

Similarly, the same approach might be used to determine the maximum percolating particle radius for a hard-sphere or soft-shell arrangement by determining the extra soft-shell thickness to block fluid percolation. For example [again using Fig. 8 and Eq. (6)], if a hard-sphere volume fraction of 0.3 is assumed, with a soft-shell thickness of $0.5r_h$, a further $0.3r_h$ thickness of the soft shell is required to block fluid percolation, hence this is also the maximum particle radius for passing through. All of this is summarized in Fig. 9, which illustrates particle size versus hard-sphere volume fraction for varying soft-shell thicknesses.

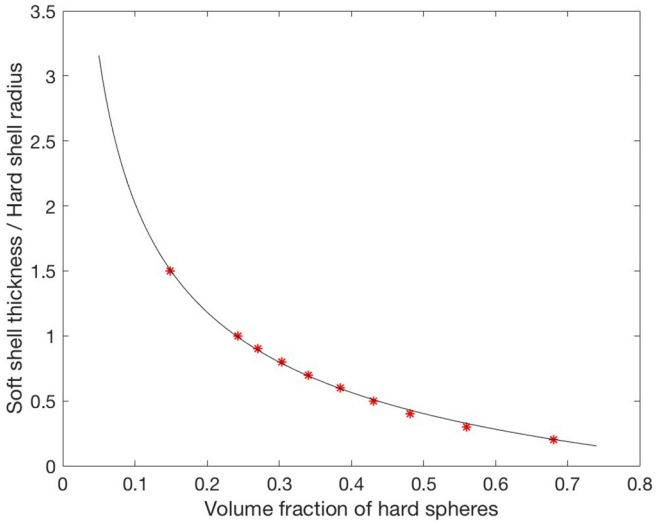

FIG. 8. Ratio of soft-shell thickness to hard-core radius to achieve the percolation threshold for a range of hard-sphere volume fractions.

While the JKS model (given in Eq. 4) has typically been applied to a hard-sphere type geometry, we apply the relation to all cases shown in Fig. 9 to identify the limitations of the analytical relationship. In order to implement the JKS model, the relationships between pore volume fraction and surface area are required. However, extracting the surface area for the geometrical models developed above turns out to be a more taxing computational task than that of computing the maximum particle size reported in Fig. 9. The MATLAB "isosurface" function was utilized to identify the relevant surface, and the resultant model regularly exceeded the 128 GB of RAM available on the supercomputer nodes during the exercise; nevertheless, a set of consistent results was obtained. The results of the two approaches are compared in Fig. 10 for several values of soft-shell thickness, with the results from this paper shown as solid lines and the JKS results shown as dotted line. As mentioned earlier, the JKS relationship is expected to be accurate for pore volume fraction $0.2 \leqslant \phi \leqslant 1$, which is the area above the black dashed line in Fig. 10 (using Fig. 7 to determine total volume fraction for a given hard-sphere volume fraction).

It can be concluded from the figure that when the porosity is high (values at the left of the figure) the JKS model overestimates the particle size that can pass through the pore space for low values of soft-shell thickness, while it underestimates the size for high values of soft-shell thickness (i.e., for soft-shell thicknesses greater than approximately 0.5 times the hard-shell radius). As the porosity decreases to 20% (the points where the solid lines cross the dashed line), the JKS model converges to the numerical data from this paper. Then as the porosity decreases below 20% (to the right of this intersection) the JKS model once again diverges from the more accurate results of this paper, each time indicating higher particle size than the numerically measured values. We note that a more accurate definition of $m(\phi)$ in Eq. (4) could improve the

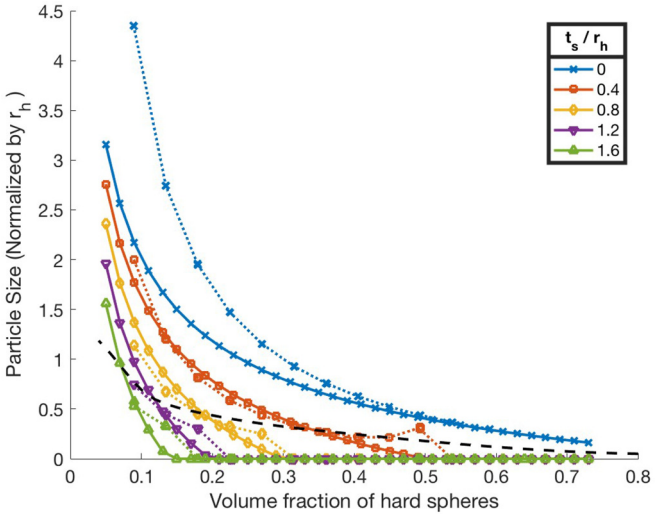

FIG. 10. Comparison between current paper particle size calculations (solid lines) and the JKS model (dotted lines) for several soft-shell thicknesses.

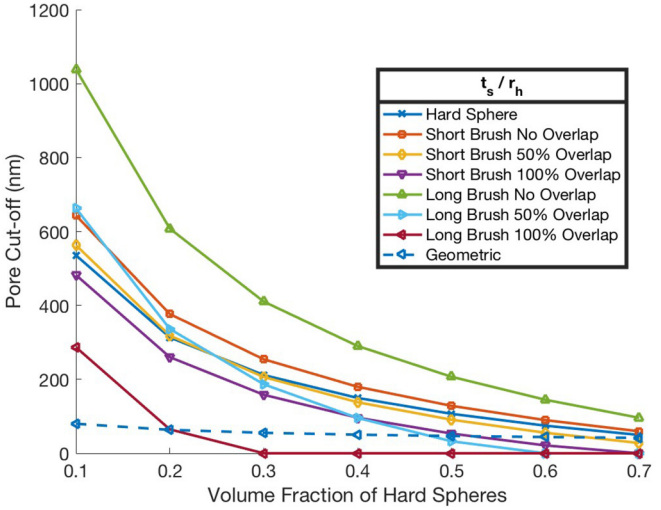

FIG. 11. Graph of the various models that can be used to estimate the particle size cutoff as a function of the silica particle size and volume fraction within the membrane.

results of the JKS model for the base case of hard spheres, but it appears that a modification would be required for the model to account for geometries represented by a hard sphere and soft shell.

Applications for hairy nanoparticle membranes

This type of analysis can now be used to calculate the percolation properties and path diameters of membranes created from silica modified with polymer brushes, a hard-core or soft-shell system. As described earlier, two types of membranes were formed with silica of mean diameter 265 ± 20 nm: one with short polymer brushes (DP 100) and the second with long polymer brushes (DP 500).

The first system to be discussed is the bare silica. Because the membrane system created is not ordered, the sphere arrangement is assumed to be random close packed with a volume fraction of 0.64 [24,25]. The calculated particle size that can pass through the system is 64.0 nm according to Eq. (6). This is 1.5 times higher than the particle size calculated through the geometric model [Eq. (2)], which was 43 nm. Adding the soft shell to the system with complete overlap of the polymers (no change in volume fraction of silica spheres) causes the maximum filtration cutoff to decrease to 10.5 nm for the short brushes and 0 nm for the long brushes, the membrane being completely nonporous in the latter case. If, on the other hand, the polymer layer simply adds to the diameter of the hard sphere, with no overlap between neighboring particles, the maximum particle sizes that can pass through and be transported through the membranes are 73.8 and 4.9 nm, respectively. These systems have been graphed in Fig. 11 for constant silica hard-sphere size of 265 nm, along with the further case of 50% overlap; the simple geometrical estimate from Eq. (2) is also shown. For high volume fractions (close to the close-packed volume fraction of 0.7405), the geometric model (green dashed line in Fig. 11) gives a reasonable estimate for the maximum particle size; however, at low volume fractions it is a very poor estimate.

Equation (6) can be modified to take into account an assumed fraction of overlap of the polymer brushes. The fraction of allowed overlap is assumed to be v_o, and it is assumed that the nonoverlapping portions of the brushes simply add to the diameter of the silica spheres and contribute to the 0.64 volume fraction; the overlapping brush sections are assumed to not be included as part of the volume fraction, in order to arrive at a simple equation. Then Eq. (6) can be rewritten as shown below, where b is the brush thickness:

$$\frac{t_s - b * v_o}{r_h + b * (1 - v_o)} = 1.1579 V_h^{-0.440} - 1.1678. \quad (7)$$

If this equation is applied to cutoff experiments for different membranes [1,19], the overlap of the brushes can be estimated (assuming that the volume fraction is known to be ~0.64). Two sizes of spheres were experimentally tested: 280- and 460-nm silica spheres, with 24- and 30-nm length brushes, respectively. The smaller spheres allowed 6-nm particles to pass through, while 20-nm particles were blocked; the larger spheres allowed 20 nm to pass through, while 40-nm particles were blocked. Hence, the cutoff size is between 6 and 20 nm for the smaller spheres, and between 20 and 40 nm for the larger spheres. In both cases the predicted allowed overlap is close to 1 (0.99 if one assumes 20-nm cutoff size for the smaller spheres, and 1.0 if the cutoff is assumed to be less than 20 nm). Hence, for these brushes, there appears to be full overlap allowed—either through interdigitation or through deformation. There may also be some other factors that contribute to the observed size selectivity, such as tortuosity effects or interactions of the diffusing species with the polymer brushes. A more interesting case would involve comparison with longer brush cutoff trials, where the brushes are more unlikely to fully overlap.

One should also keep in mind that the hard-sphere soft-shell model is an idealization of the actual situation for the hairy nanoparticles. Currently the amount of overlap of the hairy surfaces is not fully characterized, and, furthermore, the particle cutoff size may be affected by other issues such as

charging of the hairs or particles. Hence other factors must be taken into account beyond the purely geometrical idealization. Nevertheless, the current paper provides a powerful tool for assessing the geometrical aspects of the problem.

IV. CONCLUSIONS

In this paper, the maximum particle size that could pass through a random hard-core soft-shell system was calculated by considering percolation through a 3D lattice discretization of continuum sphere assemblages. The lattice-based percolation results agree well with published data [6,9]. The pass-through size calculation also agrees well with the previously published JKS model at low porosity values, but diverges somewhat at high porosity values (to the left of the graph in Fig. 10). The present results are expected to be the more accurate model, since the pass-through size is actually numerically measured in this paper, rather than being inferred from geometrical metrics and empirical observations. It should also be noted that, while the JKS model is extremely simple to express, in practice it is difficult to apply due to the complication of obtaining pore surface area. The computational cost of estimating this value was higher than that required to obtain the numerical pass-through values for this paper, although we note that there may be simpler ways to obtain this value experimentally or numerically.

This discrete pixel-based percolation model provides an easy to use and flexible tool for the study of percolation over a wide variety of cases, with validated accurate analysis of the percolation threshold for a continuous system of random spheres. It was also shown that a normal distribution of sphere sizes does not significantly change the percolation threshold, for distributions typical of manufactured spheres.

HNP membranes can be idealized as a random hard-core soft-shell system. For an assumed membrane volume fraction (typically taken to be close to 0.64), a maximum particle size that can pass through the pores can be calculated for a membrane of known silica sphere diameter and polymer brush length. It was found that the analytical geometry-based estimates of maximum particle size are reasonable for systems with high volume fractions (>0.6) but are not a good representation of systems of low volume fractions.

Comparison with cutoff experiments indicates that shorter brushes used in HNP membranes allow the polymer brushes to fully overlap with neighboring spheres (either through interdigitation or mutual deformation). This method of determining the degree of overlap requires further validation for longer brushes.

The results presented in this paper allow the calculation of the particle size cutoff for any random sphere membrane. The full MATLAB [26] code is available online [19].

ACKNOWLEDGMENTS

We thank the anonymous reviewer for pointing out the JKS model, and for other helpful comments. Funding for E.V.W. and I.Z. was provided by NSF Grant No. CHE-1710052. Funding for D.F. was provided by NSF Grant No. CMMI-1538447. K.M.G. gratefully acknowledges support from NSF Grants No. DMS-1413454 and No. DMS-1715680, and ONR Grant No. N00014-18-1-2552. Graeme Milton and Elena Cherkaev also provided invaluable insights during the development of this paper.

[1] A. Khabibullin, E. Fullwood, P. Kolbay, and I. Zharov, ACS Appl. Mater. Interfaces **6**, 17306 (2014).
[2] D. Stauffer and A. Aharony, *Introduction to Percolation Theory*, 2nd ed. (Taylor & Francis, London, 1992).
[3] G. Grimmett, *Percolation*, 2nd ed. (Springer, New York, 1999).
[4] S. Torquato, *Random Heterogeneous Materials* (Springer-Verlag, New York, 2002).
[5] I. Balberg and N. Binenbaum, Phys. Rev. A **35**, 5174 (1987).
[6] D. J. Priour, Phys. Rev. E **89**, 012148 (2014).
[7] M. D. Rintoul, Phys. Rev. E **62**, 68 (2000).
[8] M. J. Saxton, Biophys. J. **99**, 1490 (2010).
[9] N. S. Martys, S. Torquato, and D. P. Bentz, Phys. Rev. E **50**, 403 (1994).
[10] A. Oladewa, Effect of random particle size distribution on the percolation threshold of composites, M.S. thesis, University of Toledo, 2015.
[11] V. Ambegaokar, B. I. Halperin, and J. S. Langer, Phys. Rev. B **4**, 2612 (1971).
[12] K. M. Golden and S. M. Kozlov, Homogenization **50**, 21 (1999).
[13] A. J. Katz and A. H. Thompson, Phys. Rev. B **34**, 8179 (1986).
[14] V. Robins, M. Saadatfar, O. Delgado-Friedrichs, and A. P. Sheppard, Water Resour. Res. **52**, 315 (2016).
[15] D. L. Johnson, J. Koplik, and L. M. Schwartz, Phys. Rev. Lett. **57**, 2564 (1986).
[16] R. E. De La Rue and C. W. Tobias, J. Electrochem. Soc. **106**, 827 (1959).
[17] D. L. Johnson, T. J. Plona, C. Scala, F. Pasierb, and H. Kojima, Phys. Rev. Lett. **49**, 1840 (1982).
[18] E. B. W. Stöber and A. Fink, J. Coll. Interf. Sci. **26**, 62 (1968).
[19] E. V. White, Nanoporous membranes from the assembly of hairy nanoparticles, Ph.D. dissertation, University of Utah, 2019.
[20] Y. Eygeris, E. V. White, Q. Wang, J. E. Carpenter, M. Gruenwald, and I. Zharov, ACS Appl. Mater. Interfaces **11**, 3407 (2019).
[21] J. Choi, H. Dong, K. Matyjaszewski, and M. R. Bockstaller, J. Am. Chem. Soc. **132**, 12537 (2010).
[22] CHomP: Computational Homology Project, Rutgers University (2009), http://chomp.rutger.edu.
[23] D. D. Gerrard, D. T. Fullwood, D. M. Halverson, and S. R. Niezgoda, Comput. Mater. Contin. **15**, 129 (2010).
[24] G. D. Scott and D. M. Kilgour, J. Phys. D **2**, 863 (1969).
[25] S. Torquato, T. M. Truskett, and P. G. Debenedetti, Phys. Rev. Lett. **84**, 2064 (2000).
[26] MathWorks, Natick, MA, 2017.